

ACOUSTO-OPTIC MODULATION OF LIGHT

https://doi.org/10.1070/QEL17516

Acousto-optic modulation of light polarisation in monoclinic crystals

A.I. Chizhikov, N.F. Naumenko, K.B. Yushkov, V.Ya. Molchanov, A.A. Pavlyuk

Abstract. **A configuration of a laser polarisation modulator based on isotropic acousto-optic interaction is proposed. Polarisation control is performed by a 2D acousto-optic cell based on one monoclinic single crystal. A possibility of implementing this modulator on the basis of a $KY(WO_4)_2$ crystal is demonstrated.**

Keywords: *acousto-optics, polarisation, biaxial crystal, potassium-yttrium tungstate, laser Q-switch.*

1. Introduction

Acousto-optic (AO) modulators (AOMs) are widely applied in laser physics as *Q*-switches, mode lockers, ultrashort laser pulse pickers, frequency shifters, and phase stabilisers [1–6]. Generally, AOMs have an isotropic AO interaction geometry, in which polarisation of diffracted laser beam coincides with the incident beam polarisation. The AO medium can be either isotropic (glass, liquid) or anisotropic (single crystal). The AO interaction efficiency in isotropic and anisotropic media depends generally on the laser light polarisation. Polarisation-independent AOMs are often used in practice. The acousto-optic interaction efficiency of these AOMs depends weakly on the incident beam polarisation and, therefore, only slightly changes the diffracted beam polarisation. These AOMs are widely used, e.g., in fibre lasers, which are characterised by random beam polarisation. Different configurations of AO interaction are used to control laser polarisation [7–11].

In recent years, a number of new AOM configurations have been developed based on monoclinic biaxial crystals of potassium–yttrium tungstate (KYW) and potassium–gadolinium tungstate (KGW) [12–17]. These materials are characterised by a combination of fairly high AO figure of merit for isotropic diffraction and high laser-induced damage threshold, due to which they can be applied in high-power mid-IR lasers. Since the aforementioned materials are widely used as laser active media, the technology of growing their single crystals of high optical quality and necessary sizes has been well developed. Another feature of biaxial crystals making them interesting for acousto-optics is that, due to the lower symmetry of physical properties, the AO interaction geometries are more diverse than in the case of uniaxial crystals. At the same time, only biaxial crystals of orthorhombic (e.g., Tl_3AsS_4, $PbBr_2$, α-HIO_3, etc.) and monoclinic (Pb_2MoO_5, KGW, KYW) systems are used in all known applications.

The purpose of this work was to analyse the geometry of a new-type AOM allowing for controlling laser polarisation. The proposed modulator architecture is similar to that of intracavity *Q*-switch: the working beam at the output is a zero-order diffraction beam; however, in contrast to conventional AO *Q*-switches, two independent acoustic beams in one single crystal control two orthogonal laser polarisations. This type of AOM is promising for designing solid-state *Q*-switched lasers and switching the output beam polarisation.

2. Concept of polarisation modulator

The proposed configuration of an AO polarisation modulator is based on independent control of two optical eigenmodes of a birefringent crystal by two acoustic waves propagating in different directions. A schematic of the AO cell is shown in Fig. 1. It consists of two transducers, which are bonded to different faces of a single crystal and controlled independently by two rf generators. The AO interaction region is the intersection domain of bulk acoustic wave (BAW) beams in the crystal. An incident laser beam propagates, making a Bragg angle θ_{B1} with the first BAW and a Bragg angle θ_{B2} with the second BAW. At the output of the AO cell, one can observe two diffracted beams with wave vectors $\boldsymbol{k}_{d1}$ and $\boldsymbol{k}_{d2}$ along with the zero-order diffraction beam having a wave vector $\boldsymbol{k}_0$. The working output beam is the zero-order diffraction beam. The Bragg angles θ_{B1} and θ_{B2} are determined by the ultrasonic frequencies f_1 and f_2, respectively, which may generally differ. In most cases, AO modulators work at a fixed frequency of a carrier signal; therefore, from practical considerations, it is convenient to choose equal frequencies: $f_1 = f_2$. The rf signal amplitudes A_1 and A_2 are determined by the necessary diffraction efficiency. Since the AO figure of merit of a medium depends on both the laser beam polarisation and the BAW propagation direction in the crystal, the A_1 and A_2 values necessary for implementing the same diffraction efficiency differ.

A.I. Chizhikov, N.F. Naumenko, K.B. Yushkov, V.Ya. Molchanov
National University of Science and Technology MISiS, Leninsky prosp. 4, 119049 Moscow, Russia;
e-mail: konstantin.yushkov@misis.ru;
A.A. Pavlyuk Nikolaev Institute of Inorganic Chemistry, Siberian Branch, Russian Academy of Sciences, prosp. Akad. Lavrent'eva 3, 630090 Novosibirsk, Russia;
e-mail: pavlyuk@niic.nsc.ru

Received 24 December 2020
Kvantovaya Elektronika **51** (4) 343–347 (2021)
Translated by Yu.P. Sin'kov

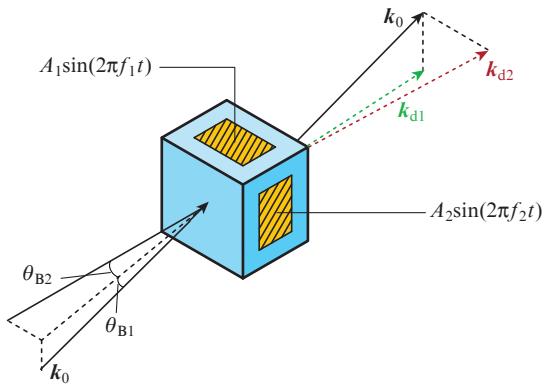

Figure 1. (Colour online) Schematic of the AO cell of a polarisation modulator.

Further analysis will be performed in a monoclinic crystal system. We will use a standard system of axes in monoclinic crystals, where the twofold symmetry axis is parallel to the X_2 axis. The vector diagram of AO interaction is shown in Fig. 2. The X_1, X_2, and X_3 axes are the principal axes of the permittivity tensor. A laser beam with a wave vector $\boldsymbol{k}_0$ propagates near the crystal symmetry axis X_2. Let the beam polarisation be arbitrarily oriented relative to the X_1 and X_3 axes. In the crystal the beam is divided into fast and slow modes with wave vectors $\boldsymbol{k}_f$ and $\boldsymbol{k}_s$, respectively. The polarisation of eigenmodes is set by the vectors $\boldsymbol{D}_f || X_1$ and $\boldsymbol{D}_s || X_3$,

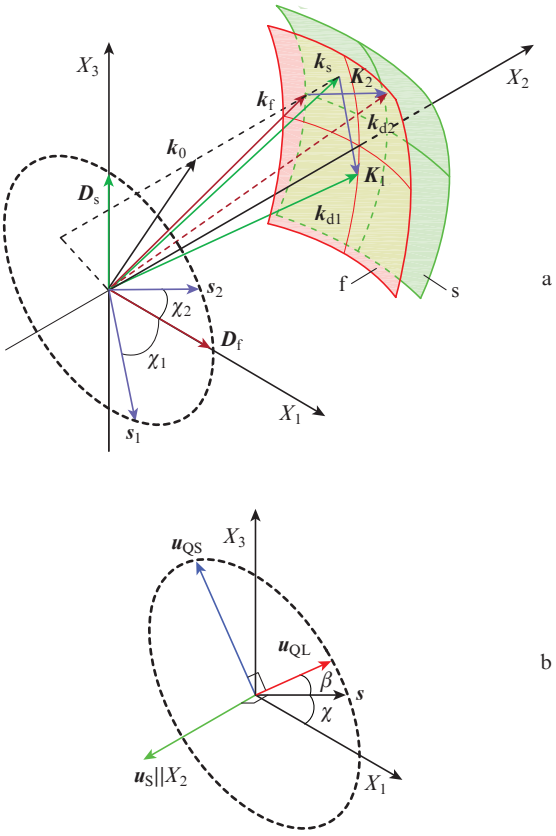

Figure 2. (Colour online) (a) Vector diagram of AO interaction in a polarisation modulator and (b) directions of BAW displacement vectors in the crystal symmetry plane.

respectively. Fragments of the optical surfaces of wave normals in Fig. 2 are denoted by letters f and s. The BAW wave vectors $\boldsymbol{K}_1$ and $\boldsymbol{K}_2$ and the corresponding unit vectors $\boldsymbol{s}_1$ and $\boldsymbol{s}_2$ lie in the X_1X_3 plane. The BAW propagation direction ($\boldsymbol{s}$ vector) will be set by the angle χ, counted relative to the X_1 axis and ranging from –90° to 90°. Since X_1X_3 is a symmetry plane of the crystal, one of the BAW modes is a pure shear mode with a displacement vector $\boldsymbol{u}_S || X_2$. The effective photoelastic constant of isotropic AO diffraction for this wave is always zero. Two other BAW modes, quasi-longitudinal and quasi-shear, are polarised in the X_1X_3 plane. The directions of their displacement vectors $\boldsymbol{u}_{QL}$ and $\boldsymbol{u}_{QS}$ will be set by the polarisation angle β between the $\boldsymbol{s}$ and $\boldsymbol{u}_{QL}$ vectors, as shown in Fig. 2b.

3. Analysis of the AO effect in monoclinic crystals

A necessary condition for controlling the polarisation state of an output laser zero-order diffraction beam is the independence of AO interaction for two eigenpolarisations of crystal. This condition can be implemented if the BAW propagation directions in the AO crystal are chosen so that the effective photoelastic constant for the fast eigenmode is zero in the case of BAW propagation in the direction of the unit vector $\boldsymbol{s}_1$ and the photoelastic constant for the slow eigenmode is zero when a BAW propagates in the direction of the unit vector $\boldsymbol{s}_2$. Furthermore we will consider the possibility of implementing these conditions.

Different designations are used in the literature for the principal axes of the permittivity tensor ε of biaxial crystals. In KYW and KGW crystals, in the chosen setting of the axes, $\varepsilon_{22} < \varepsilon_{11} < \varepsilon_{33}$; i.e., the X_1 and X_3 axes correspond to the N_m and N_g axes, respectively. The effective photoelastic constants of AO interaction are expressed in terms of the photoelastic tensor components p_{ij} in the Voigt notation for the quasi-longitudinal BAW mode as

$$p_{QL} = p_{\alpha 1}\cos\chi\cos(\chi+\beta) + p_{\alpha 3}\sin\chi\sin(\chi+\beta) + p_{\alpha 5}\sin(2\chi+\beta) = \frac{p_{\alpha 1}+p_{\alpha 3}}{2}\cos\beta + \frac{p_{\alpha 1}-p_{\alpha 3}}{2}\cos(2\chi+\beta) + p_{\alpha 5}\sin(2\chi+\beta) \quad (1)$$

and for the quasi-shear BAW mode as

$$p_{QS} = -p_{\alpha 1}\cos\chi\sin(\chi+\beta) + p_{\alpha 3}\sin\chi\cos(\chi+\beta) + p_{\alpha 5}\cos(2\chi+\beta) = -\frac{p_{\alpha 1}+p_{\alpha 3}}{2}\sin\beta - \frac{p_{\alpha 1}-p_{\alpha 3}}{2}\sin(2\chi+\beta) + p_{\alpha 5}\cos(2\chi+\beta), \quad (2)$$

where $\alpha = 1$ sets the constant p_f for the fast optical eigenmode with $\boldsymbol{D}_f || X_1$, and $\alpha = 3$ sets the constant p_s for the slow optical eigenmode with $\boldsymbol{D}_s || X_3$. Thus, the effective constants p_{QL} and p_{QS} for each eigenpolarisation are determined by three independent components of the photoelasticity tensor.

Expressions (1) and (2) for the photoelastic constants are exact, but one must take into account that the BAW polarisation angle β also depends on the angle χ. Nevertheless, the β value is generally sufficiently small (in particular, it does not exceed 11° and 12° in the KGW and KYW crystals, respectively), due to which the main regularities of changes in p_{QL} and p_{QS} can be revealed on the assumption that $\beta = 0$. In

this approximation the p_{QL} value has a bias $(p_{\alpha 1} + p_{\alpha 3})/2$, and there may be no zeros of the function $p_{QL}(\chi)$. In contrast, the p_{QS} value does not has this bias, and its zeros can be found from the formula

$$\chi \approx 0.5 \arctan \frac{2p_{\alpha 5}}{p_{\alpha 1} - p_{\alpha 3}} + \frac{\pi}{2} m, \; m \in \mathbb{Z}. \tag{3}$$

Expression (3) describes the approximate positions of zeros of the function $p_{QS}(\chi)$ at $\beta = 0$.

The results of calculating the $p_{QS}(\chi)$ values in the case $\beta \neq 0$ and the corresponding values of AO figure of merit M_2 are shown in Figs 3a and 3b. Furthermore the angle χ_1 is determined by the condition $p_f = 0$ for the fast optical eigenmode, and the angle χ_2 is determined by the condition $p_s = 0$ for the slow optical eigenmode. There are two different zeros of the function $p_{QS}(\chi)$, spaced by ~90°, for each polarisation; however, when using an AO modulator, it is preferred to have a difference between the angles χ_1 and χ_2 close to 90° for independent tuning of the Bragg angles θ_{B1} and θ_{B2}. Calculations were performed with the elastic and photoelastic constants of crystals taken from [12–14].

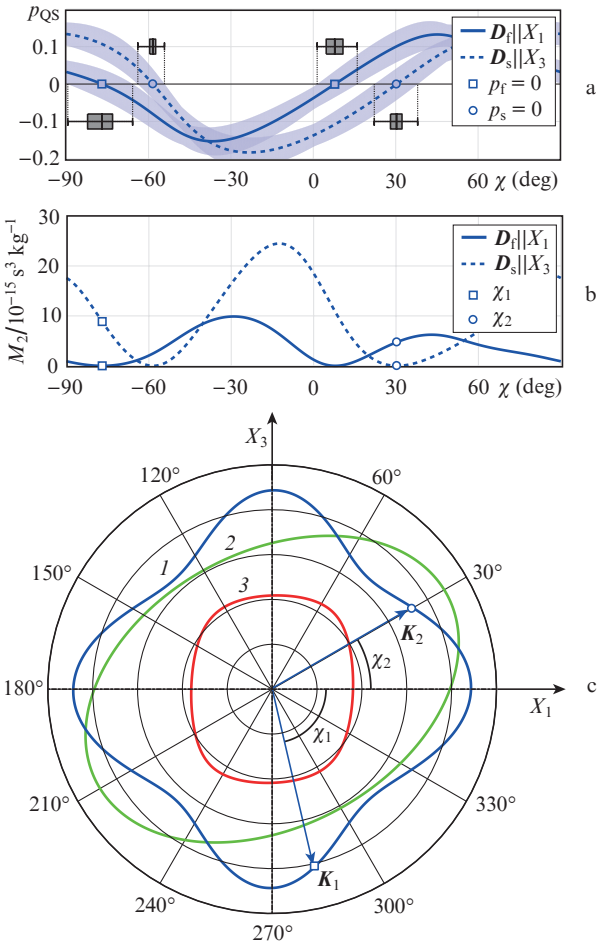

Figure 3. (Colour online) (a, b) Characteristics of isotropic diffraction in the symmetry plane of a KYW crystal for a quasi-shear BAW mode: (a) effective photoelastic constant p_{QS} with confidence intervals and (b) AO figure of merit M_2 (c). Cross section of the BAW slowness surface and the wave vectors corresponding to zeros of the $p_{QS}(\chi)$ function for different light polarisations. Curves (*1*), (*2*), and (*3*) correspond, respectively, to the quasi-shear, shear, and quasi-longitudinal modes.

An important factor determining the error in finding the angles χ_1 and χ_2 is the error in measuring the photoelastic constants. We assume the absolute error to be invariable for all constants and equal to 0.03, which corresponds to a relative measurement error of ~10% for the constants maximum in magnitude [13, 14]. As follows from expression (3), the maximum values of χ_1 and χ_2 are implemented at the maximum value of $|p_{\alpha 5}|$ and minimum value of $|p_{\alpha 1} - p_{\alpha 3}|$ within the confidence interval of photoelastic constants. Similarly, the minimum values of χ_1 and χ_2 are implemented at the minimum value of $|p_{\alpha 5}|$ and maximum value of $|p_{\alpha 1} - p_{\alpha 3}|$. The calculated effective photoelastic constants p_{QS} in Fig. 3a are shown taking into account the confidence intervals (hatched regions) calculated by the Monte Carlo method. Based on the calculations performed, one can find two possible configurations of an AO polarisation modulator, whose characteristics for the KYW and KGW crystals are listed in Table 1. The values of angles χ_1 and χ_2 are indicated with confidence intervals (in square brackets), which were determined as the 0.25th and 0.75th quantiles of possible positions of zeros of the functions $p_f(\chi)$ and $p_s(\chi)$. Figure 3a shows also the distribution quartiles for each of the points $p_{QS} = 0$.

Table 1. Parameters of configurations of AO polarisation modulators based on KYW and KGW crystals.

Crystal	Configuration	χ_1	χ_2	$M_2/10^{-15}$ s^3 kg^{-1}	
				$\boldsymbol{D}_f\|\|X_1$	$\boldsymbol{D}_s\|\|X_3$
KYW	1	–77° [–82.2°, –73.1°]	+30° [28.1°, 32.3°]	4.6	7.6
	2	+8° [4.7°, 9.8°]	–58° [–59.6°, –57.4°]	2.5	9.4
KGW	1	–67° [–70.8°, –64.8°]	+27° [25.2°, 29.7°]	0.8	1.1
	2	+16° [11.3°, 19.5°]	–61° [–62.5°, –60.1°]	0.3	2.9

As follows from the presented results, the zeros of the functions $p_f(\chi)$ and $p_s(\chi)$ for orthogonal light polarisations in the KGW crystal are located closer to each other than in the KYW crystal, as a result of which the values of AO figure of merit M_2 are much smaller. Based on this, we can conclude that the KYW crystal is more preferred for designing a laser polarisation modulator as compared with the KGW crystal. In the KYW crystal, for configuration 1, the total BAW power is about 30% lower than that for configuration 2. The wave vectors $\boldsymbol{K}_1$ and $\boldsymbol{K}_2$ form an angle of 107°, as shown in Fig. 3c.

4. Results and discussion

As was demonstrated above, the existence of geometries of isotropic AO interaction in the symmetry plane of monoclinic crystals for selective control of the intensity of orthogonally polarised optical eigenmodes is due not to a random coincidence of effective photoelastic constants but to the regularities of AO effect, with allowance for the symmetry of crystal physical properties. Let us consider the possibility of existence of similar AO geometries of interaction in crystals belonging to other systems.

The symmetry properties of the classes 32, 3m, and $\bar{3}$m of a trigonal system are most similar to those of a monoclinic

system. Examples of AO crystals belonging to these classes are quartz, lithium niobate, and α-BBO (BaB_2O_4). In this case, the symmetry plane is the X_2X_3 plane, which corresponds to the YZ plane; the ordinary wave is polarised along the X_2 axis, corresponding to the Y axis ($\alpha = 2$); and the extraordinary wave is polarised along the X_3 axis, corresponding to the Z axis ($\alpha = 3$). For trigonal crystals, similar to (1) and (2), one can write the expressions

$$p_{QL} = p_{\alpha 2}\cos\chi\cos(\chi + \beta) + p_{\alpha 3}\sin\chi\sin(\chi + \beta) + p_{\alpha 4}\sin(2\chi + \beta), \quad (4)$$

$$p_{QS} = -p_{\alpha 2}\cos\chi\sin(\chi + \beta) + p_{\alpha 3}\sin\chi\cos(\chi + \beta) + p_{\alpha 4}\cos(2\chi + \beta). \quad (5)$$

The difference is as follows: the p_{QS} value for an ordinary wave is determined by only two independent photoelastic constants, because $p_{34} = 0$. As a result, the angle β affects significantly the positions of zeros of the p_{QS} function, and the expression of type (3) becomes inapplicable for approximate determination of these zeros.

In crystals belonging to other systems (except for the triclinic system, which is not considered here because of the absence of known AO materials), the effective photoelastic constants p_{QL} and p_{QS} for each optical eigenmode are determined by only two independent constants, because $p_{\alpha 4} = p_{\alpha 5} = 0$. As a result, the function $p_{QL}(\chi)$ has no zeros at all, and the function $p_{QS}(\chi)$ is always zero for both light polarisations along the symmetry axes, i.e., at $\chi = 0$ and at $\chi = 90°$. There also may be intermediate points $p_{QS}(\chi) = 0$ which are determined by both the ratio of nonzero constants and the BAW polarisation angle β.

The configuration of AO interaction under consideration can be used to design laser Q-switches controlling the light polarisation in cavities with weak amplitude anisotropy. In the absence of polarisation-selective elements, bistable and random regimed of generation of orthogonally polarised radiation may occur in these lasers [18, 19]. One of the ways to control the light polarisation in these lasers is to use the pump beam polarisation; however, a significant delay between the switchings of the pump polarisation direction and the change in output polarisation may arise in this case [20].

The AO Q-switch proposed in this study, which is based on a KYW crystal with two acoustic channels, controlling independently the intensity of orthogonal crystal eigenmodes, makes it possible to modulate independently the cavity Q factor for two polarisations and, therefore, switch the output beam polarisation. Both acoustic beams are switched on in the closed state of the Q-switch. When one of the beams is switched off, the loss for the corresponding polarisation decreases to a level below the threshold, and generation of linearly polarised light may occur. The cavity remains closed for the orthogonal polarisation. The polarisation switching is accompanied by a frequency shift between the independent modes with mutually orthogonal polarisations because of the phase anisotropy introduced into the cavity by the birefringent crystal. For the chosen angles $\chi_1 = 30°$ and $\chi_2 = -77°$ in the KYW crystal the ultrasonic velocities are, respectively, 2760 and 2445 m s^{-1}. Thus, the difference in the switching rates for two polarisations is small: 12%. At the same time, the ultrasonic velocities in this crystal are lower by a factor of about two than in quartz, a factor reducing the Q-switch angular selectivity and allowing one to control radiation in cavities with a complex structure of transverse modes.

Let us estimate the consumed power for an AO Q-switch based on the chosen configuration of the KYW crystal. A conventional material for AO Q-switches is crystalline quartz, for which $M_2 = 1.6 \times 10^{-15}$ s^3 kg^{-1} in the case where a laser beam propagating along the Z axis is diffracted by a longitudinal BAW. For a wavelength of 1064 nm, the typical consumed power of these AO Q-switches is ~30 W at a diffraction efficiency of no less than 80%. The isotropic-diffraction efficiency greatly exceeding that for quartz makes it possible to design more compact laser Q-switches based on KYW and KGW crystals, which consume power as low as several watts and operate at wavelengths up to 3 μm [15–17]. The M_2 value for the configurations of AO interaction in the KYW crystal that were found in this study are larger by factor of about three and five than that for quartz. Therefore, even at a simultaneous switching on of two acoustic waves, their total power will be ~15 W for a wavelength of 1064 nm at the same sizes of piezoelectric transducers as and in a quartz-based AO Q-switch (aperture ~2 mm, interaction length ~40 mm).

5. Conclusions

It was shown that there is a geometry of isotropic AO interaction in monoclinic crystals in which two ultrasonic beams with different directions of wave vectors in one single crystal allow one to modulate independently the intensities of fast and slow optical eigenmodes propagating along the crystal symmetry axis. It follows from the calculations that the AO figure of merit in the KYW crystal for this geometry is 4.6×10^{-15} s^3 kg^{-1} for the light polarised along the X_1 axis (N_m axis) and 7.6×10^{-15} s^3 kg^{-1} for the light polarised along the X_3 axis (N_g axis); these values exceed several times the AO figure of merit of crystalline quartz. The proposed AO interaction geometry is promising for designing new-type laser Q-switches.

Acknowledgements. This work was supported by the Russian Foundation for Basic Research (Grant No. 20-07-00115).

References

1. Koke S., Grebing S., Frei H., Anderson A., Assion A., Steinmeyer G. *Nat. Photonics*, **4**, 462 (2010).
2. Gulyaev Yu.V., Kazaryan M.A., Mokrushin Yu.M., Shakin O.V. *Quantum Electron.*, **45**, 283 (2015) [*Kvantovaya Elektron.*, **45**, 283 (2015)].
3. De Vries O., Saule T., Plotner M., Lucking F., Eidam T., Hoffmann A., Klenke A., Hadrich S., Limpert J., Holzberger S., Schreiber T., Eberhardt R., Pupeza I., Tunnermann A. *Opt. Express*, **23**, 19586 (2015).
4. Aldous M., Woods J., Dragomir A., Roy R., Himsworth M. *Opt. Express*, **25**, 12830 (2017).
5. Nanii O.E., Odintsov A.I., Panakov A.I., Smirnov A.P., Fedoseev A.I. *Quantum Electron*, **49**, 119 (2019) [*Kvantovaya Elektron.*, **49**, 119 (2019)].
6. Slinkov G.D., Mantsevich S.N., Balakshy V.I., Magdich L.N., Machikhin A.S. *IEEE Trans. Ultrason. Ferroelectr. Freq. Control*, **67**, 1242 (2020).
7. Antonov S.N., Kotov V.M., Sotnikov V.N. *Sov. Phys. Tech. Phys*, **36**, 101 (1991) [*Zh. Tekh. Fiz.*, **61** (1), 168 (1991)].
8. Gondek G., Kwiek P. *Ultrasonics*, **40**, 967 (2002).

9. Antonov S.N. *Tech. Phys*., **49**, 1329 (2004) [*Zh. Tekh. Fiz*., **74** (10), 84 (2004)].
10. Yushkov K.B., Molchanov V.Ya., Chizhikov S.I. RF Patent No. 2613943 (priority date March 22, 2017).
11. Kotov V.M., Averin S.V., Kotov E.V., Voronko A.I., Tikhomirov S.A. *Quantum Electron*., **47**, 135 (2017) [*Kvantovaya Elektron*., **47**, 135 (2017)].
12. Mazur M.M., Velikovskiy D.Yu., Mazur L.I., Pavluk A.A., Pozhar V.E., Pustovoit V.I. *Ultrasonics*, **54**, 1131 (2014).
13. Mazur M.M., Mazur L.I., Pozhar V.E. *Tech. Phys. Lett*., **41**, 249 (2015) [*Pis'ma Zh. Tekh. Fiz*., **41** (5), 91 (2015)].
14. Mazur M.M., Mazur L.I., Pozhar V.E. *Physics Procedia*, **70**, 741 (2015).
15. Mazur M.M., Mazur L.I., Pozhar V.E., Shorin V.N., Konstantinov Yu.P. *Quantum Electron*., **47**, 661 (2017) [*Kvantovaya Elektron*., **47**, 661 (2017)].
16. Yushkov K.B., Chizhikov A.I., Naumenko N.F., Molchanov V Ya., Pavlyuk A.A., Makarevskaya E.V., Zakharov N.G. *Proc. SPIE*, **10899**, 1089913 (2019).
17. Pushkin A.V., Mazur M.M., Sirotkin A.A., Firsov V.V., Potemkin F.V. *Opt. Lett*., **44**, 4837 (2019).
18. Zolotoverkh I.I., Lariontsev E.G. *Quantum Electron*., **34**, 727 (2004) [*Kvantovaya Elektron*., **34**, 727 (2004)].
19. Cheng H.P., Huang T.L., Lee C.Y., Sung C.L., Cho C.Y., Chen Y.F. *Opt. Express*, **24**, 23829 (2016).
20. Verschaffelt G., Van der Sande G., Danckaert J., Segard B., Glorieux P., Erneux T. *Phys. Rev. A*, **77**, 063801 (2008).